

METAMORPHIC REACTIONS AND PRELIMINARY *P-T* ESTIMATES OF
ULTRAHIGH-TEMPERATURE MAFIC GRANULITE FROM TONAGH ISLAND
IN THE NAPIER COMPLEX, EAST ANTARCTICA

Toshiaki TSUNOGAE¹, Yasuhito OSANAI², Tsuyoshi TOYOSHIMA³,
Masaaki OWADA⁴, Tomokazu HOKADA⁵ and Warwick A. CROWE⁶

¹*Faculty of Education, Shimane University, Nishi Kawatsu, Matsue 690-8504*

²*Faculty of Education, Okayama University, Tsushima-naka 3-chome, Okayama 700-8530*

³*Faculty of Science, Niigata University, Ikarashi 2-chome, Niigata 950-2181*

⁴*Faculty of Science, Yamaguchi University, Yoshida 1677-1, Yamaguchi 753-8512*

⁵*Department of Polar Science, School of Mathematical and Physical Sciences, The
Graduate University for Advanced Studies, Kaga 1-chome, Itabashi-ku, Tokyo 173-8515*

⁶*Department of Geology and Geophysics, University of Western Australia, Nedlands,
Perth, WA 6907, Australia*

Abstract: Metamorphic reactions and *P-T* conditions of mafic granulites from Tonagh Island in the Archean Napier Complex were examined to evaluate the nature of mafic granulite which has suffered ultrahigh-temperature (UHT) metamorphism. Although a peak mineral assemblage is preserved in plagioclase-orthopyroxene-clinopyroxene mafic granulites, initial mineral chemistry was completely reset by retrograde metamorphism. Evidence of UHT metamorphism was therefore inferred using lamella-bearing pyroxenes as 900 to 980°C.

Hornblende-quartz, biotite-quartz, and garnet-hornblende-quartz coronas around ortho- and clinopyroxenes in two-pyroxene mafic granulites are typical evidence of retrograde metamorphism in amphibolite-facies conditions. The textures suggest that the retrograde event took place in the presence of H₂O-bearing fluid. Garnet-quartz corona after pyroxenes is another predominant texture of retrograde metamorphism throughout the studied area. As the corona is characterized by anhydrous mineral assemblages, we suggest that retrograde infiltration of H₂O-bearing fluid is a local event. The corona texture suggests that retrograde metamorphism has taken place almost isobarically, because a univariant line of the corona-forming reaction shows a gentle slope in *P-T* space. The isobaric cooling temperature (650–700°C at 6.5–8.0 kbar) is, however, significantly lower than the previously reported cooling temperature of approximately 950°C subsequent to UHT metamorphism. Mafic granulites therefore preserve the second isobaric cooling event, which is distinguished from high-temperature isobaric cooling.

The mafic granulites were subsequently intruded by mafic dykes which were also metamorphosed. *P-T* conditions recorded in the rocks are 630–670°C at 6.4–8.2 kbar, consistent with the retrograde event of host mafic granulites. The event marks the last stage of regional metamorphism recorded in mafic granulites.

key words: mafic granulite, metamorphism, Tonagh Island, Archean Napier Complex, East Antarctica

1. Introduction

The Napier Complex of Enderby Land, East Antarctica, is an example of late-Archean high-grade terrane which has suffered granulite-facies metamorphism at temperature higher than 1000°C (*e.g.* ELLIS, 1980; HARLEY, 1985; SHERATON *et al.*, 1987). The Amundsen Bay area located in the western part of the Napier Complex is known as the highest grade region of the complex where sapphirine-quartz and osumilite-bearing mineral assemblages are common (SHERATON *et al.*, 1987). Presence of orthopyroxene-sillimanite-garnet in pelitic gneiss (SHERATON *et al.*, 1987) and inverted pigeonite in meta-ironstone and mafic to intermediate granulites (SANDIFORD and POWELL, 1986; HARLEY, 1987) also support the evidence of ultrahigh-temperature (UHT) metamorphism. Although the *P-T* history of UHT metamorphic rocks has been discussed using mineral assemblages in aluminous and pelitic granulites, detailed petrological studies on UHT mafic granulite are limited to several works done by ELLIS and GREEN (1985) and HARLEY (1985) because of its monotonous mineral assemblage.

In this study we examined petrographical characteristics of mafic granulites from Tonagh Island, which is located in the southern portion of Amundsen Bay (Fig. 1).

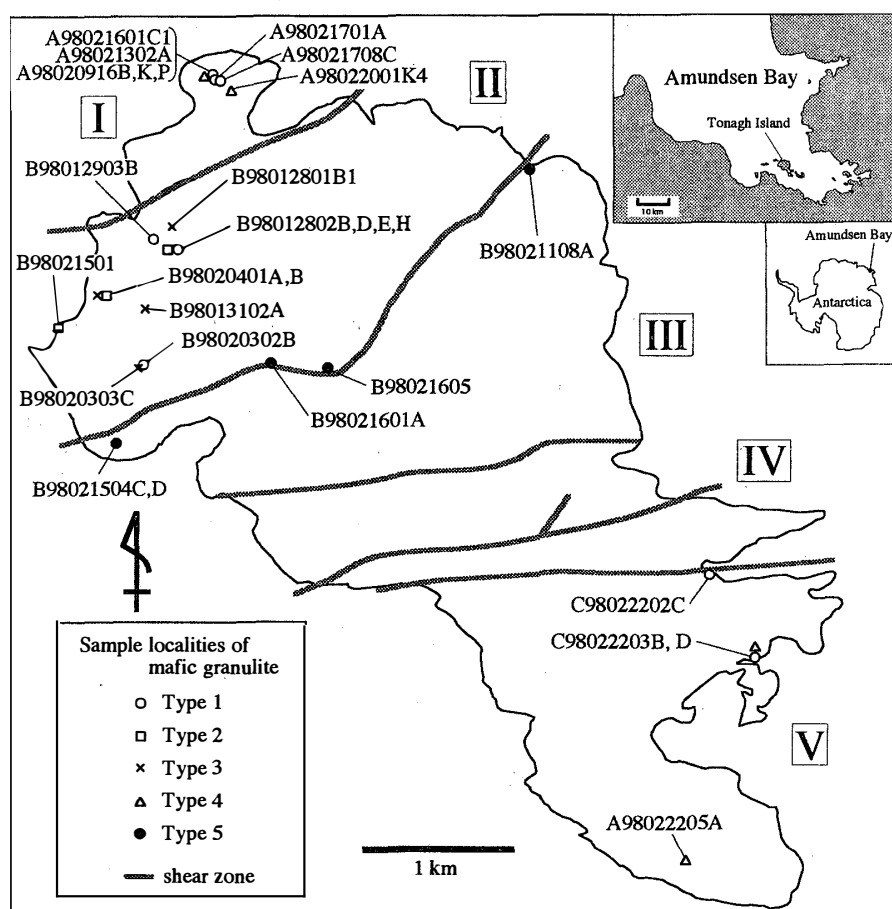


Fig. 1. Location map of Tonagh Island with localities of representative samples of mafic granulite discussed in this study. I to V denote crustal units separated by shear zones after OSANAI *et al.* (1999). Types of mafic granulite are discussed in the text.

Mafic granulite is a common lithology in the studied area. We therefore discuss mineral assemblages, reaction textures, and preliminary P - T conditions to evaluate the nature of UHT mafic granulite. The metamorphic P - T path based on detailed chemical analyses of minerals will be discussed elsewhere.

2. Brief Geology of Tonagh Island

Regional geological and structural characteristics of Tonagh Island are discussed in OSANAI *et al.* (1999). Generally the island is composed of layered gneisses of various types of rock chemistry. Orthopyroxene-bearing quartzofeldspathic gneiss is the most abundant lithology in the area. It commonly interlayers with mafic granulite, garnet-bearing felsic gneiss, and magnetite-quartz gneiss. Ultramafic granulite is present as thin layers or lenses in quartzofeldspathic and mafic granulites.

The high-grade rocks from Tonagh Island are subdivided into five crustal units (Units I to V) by high-angle and ENE-WSW to E-W trending shear zones (OSANAI *et al.*, 1999; TOYOSHIMA *et al.*, 1999). Approximate positions of the shear zones are shown in Fig. 1. Unit I corresponds to the northwestern portion of the island. There occur layered gneisses which vary in thickness from several to several tens of centimeters. Thick layers of mafic granulite (up to 100 m in thickness) are present in Units II, III, and IV. Unit V is different from the other units because of the wide occurrence of quartzofeldspathic and garnet-bearing felsic gneisses. In this study, samples from Units I, II, and V are discussed in detail because of the abundant samples of mafic granulite available from the units.

3. Petrography and Mineral Reactions

About 40 samples of mafic granulite from Tonagh Island were examined to describe mineral assemblages and metamorphic reaction textures under the microscope. Localities of representative samples are shown in Fig. 1. In this study, the term “mafic granulite” denotes pyroxene- and/or hornblende-bearing basic high-grade gneisses with more than 20 vol% plagioclase. Ultramafic granulite (less than 5 vol% plagioclase), pyroxene-bearing quartzofeldspathic gneiss (charnockite or enderbite), and garnet-orthopyroxene gneiss (plagioclase- and clinopyroxene-free) are not discussed in this study. Mineral assemblages with approximate modal abundance of minerals for representative samples are summarized in Table 1. Five distinct rock types were recognized. Types 1 to 4 are present as layered gneisses with quartzofeldspathic and garnet-bearing gneisses (Fig. 2a), while type 5 occurs as a metamorphosed mafic dyke locally cutting regional foliation of layered gneisses (Fig. 2b). Petrography and mineral reactions of individual rock types are discussed below. Mineral abbreviations are after KRETZ (1983).

Chemical analyses of minerals were performed by electron microprobe analyzer at the Research Center of Coastal Lagoon Environments, Shimane University, using an automated JEOL JXA-8800 instrument. The data were obtained under conditions of 15 kV accelerating voltage, using data processing by an Oxide-ZAF model correction program supplied by JEOL. Compositions of minerals in representative samples discussed in this study are shown in Table 2. Mineral assemblages of representative

Table 1. Approximate modal abundances of minerals in mafic granulite from Tonagh Island, Napier Complex.

Sample	Unit	Rock Type	Primary minerals										Secondary (retrograde) minerals							
			Pl	Qtz	Opx	Cpx	Hbl	Grt	Bt	Kfs	Ilm	Mag	Qtz	Pl	Cpx	Hbl	Grt	Bt		
A98020916P	I	1	⊙	×	○	○					×		×							
A98021302A	I	1	○	×	○	△					×		×							×
A98021701A	I	1	⊙	×	○	△					△		×							×
A98021708C	I	1	⊙	×	○	△					△		×							×
A98020916B	I	4	⊙	×	○	△							×		×	×			△	
A98020916K	I	4	○	×	○	△							×		×	×			△	×
A98021601C1	I	4	⊙	△	○	○					×		×		×	×			×	×
A98022001K4	I	4	⊙	×	○	△					×		×		×	×			△	×
B98012802D	II	1	⊙	×	○	△							×							×
B98012802E	II	1	⊙	△	○	○							×				×			×
B98020302B	II	1	⊙	×	○	○							×							×
B98012903B	II	1	⊙	×	○	○							×	×			×			×
B98012802H	II	2	⊙	×	△	△					△		×				○			×
B98020401A	II	2	⊙	△	△	△					×		△				⊙			
B98021501	II	2	⊙	○	○	△					△		△				△			△
B98012801B1	II	3	⊙	○	△	△							△				⊙		△	×
B98013102A	II	3	⊙	×	△	△					×						△		×	×
B98020303C	II	3	⊙	×	○	△					×		△				△		○	×
B98020401B	II	3	○	×	○	○							△				△		○	×
C98022202C	V	1	⊙	△	○	△							×							×
C98022203D	V	1	⊙	△	△	×							×							
A98022205A	V	4	⊙	×	○	△									×	×	×	×	×	×
C98022203B	V	4	⊙	△	○	△							×		×	×			×	×
B98021108A	II, III	5	○	×	×	△	△	△	×				×							
B98021504C	II, III	5	○	×	×	△	△	△	×				×							
B98021504D	II, III	5	○	×	×	△	△	△	×				×							
B98021601A	II, III	5	⊙	×	×	△	⊙	△	△				×							
B98021605	II, III	5	⊙	×	×	△	⊙	△	△				×							

⊙: abundant, ○: common, △: rare, ×: accessory

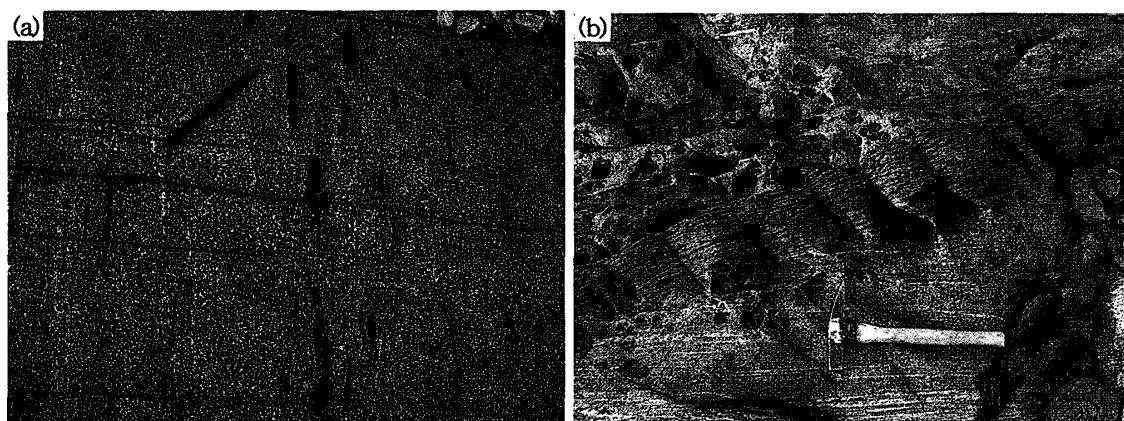


Fig. 2. Field occurrences of some mafic granulites discussed in this study.
 (a) Outcrop of mafic granulite (locality B98012802) discussed in this study. Orthopyroxene-rich lenses are common along a foliation of the granulites.
 (b) Outcrop of fine-grained metamorphosed mafic dyke (type 5 mafic granulite) which cuts the foliation of quartzofeldspathic gneiss. Pinkish elongated lenses in the dyke are rich in garnet, while the dark greenish matrix part is rich in hornblende. The outcrop is about 50 m northeast of locality B98021504 (Fig. 1).

mafic granulites and their compositions are shown in ACF diagrams (Fig. 3).

3.1. Type 1: Two-pyroxene mafic granulite (without retrograde texture)

Two-pyroxene mafic granulite is a dominant rock type throughout the studied area. It shows medium-grained granoblastic texture and is characterized by anhydrous mineral assemblages of plagioclase, orthopyroxene, and clinopyroxene (Fig. 4a). As shown in the ACF diagram (Fig. 3), the three minerals coexist together. Accessory minerals are ilmenite, magnetite, biotite, and hornblende. Sample A98020916P from a mylonite zone of Unit I shows strong mineral lineations, whereas the mineral assemblage and modal abundance of minerals in the sample are similar to those of undeformed type 1 mafic granulites.

Ortho- and clinopyroxenes occur as medium-grained subhedral crystals. They generally lack inclusions, but thin orthopyroxene lamellas are present in clinopyroxene, while orthopyroxene contains lamellas of clinopyroxene. The exsolution textures are common in mafic granulites of types 1 to 4. Ortho- and clinopyroxenes also contain thin lamellas of ilmenite as a product of exsolution during cooling. The ilmenite lamellas are generally abundant in cores of pyroxenes but are less abundant toward rims (Fig. 4b). Orthopyroxene is compositionally classified as hypersthene. Its X_{Mg} ($Mg/[Fe+Mg]$) is 0.50–0.66 but is low in sample A98021708C, only 0.35–0.37. Al content varies from sample to sample as 0.04–0.16 (based on 6 oxygens), and is generally higher at cores than rim for all samples. X_{Mg} of clinopyroxene is higher than that of orthopyroxene as 0.68–0.78. Al and Na contents in clinopyroxene is generally low as 0.08–0.18 and 0.02–0.05, respectively. There is little compositional differences between primary orthopyroxenes and orthopyroxene lamella in clinopyroxene. Lamella clinopyroxene in orthopyroxene also shows composition similar to primary clinopyroxene.

Plagioclase is a clear mineral and shows little evidence of later alteration. Anorthite

Table 2. Representative electron microprobe analyses of minerals

orthopyroxene (number of oxygens = 6)									
Sample No.	A98021701A	B98012802D	B98012802H	B98020303C	A98022001K4	A98020916K	A98020916K	B98021108A	
Rock type	Type 1	Type 1	Type 2	Type 3	Type 4	Type 4	Type 4	Type 5	
					host		lamella in Cpx		
SiO ₂	51.010	52.127	50.980	51.119	52.019	50.439	51.397	51.451	
Al ₂ O ₃	1.478	1.302	1.365	0.952	1.839	0.840	0.529	0.509	
TiO ₂	0.038	0.035	0.008	0.021	0.014	0.046	0.044	0.034	
Cr ₂ O ₃	0.135	0.017	0.023	0.000	0.009	0.101	0.071	0.000	
FeO*	25.293	25.299	28.762	29.735	22.835	29.262	28.133	32.073	
MnO	0.373	0.267	0.706	0.564	0.471	0.813	0.594	0.222	
MgO	19.567	19.396	17.424	17.527	22.511	17.032	17.968	15.771	
CaO	0.418	0.909	0.430	0.397	0.313	0.453	0.490	0.385	
Na ₂ O	0.012	0.000	0.089	0.000	0.029	0.002	0.000	0.035	
K ₂ O	0.034	0.056	0.000	0.028	0.042	0.048	0.058	0.054	
ZnO	0.042	0.000	0.104	0.033	0.038	0.011	0.031	0.115	
Total	98.400	99.408	99.891	100.376	100.120	99.047	99.315	100.649	
Si	1.962	1.981	1.965	1.968	1.941	1.970	1.986	1.993	
Al	0.067	0.058	0.062	0.043	0.081	0.039	0.024	0.023	
Ti	0.001	0.001	0.000	0.001	0.000	0.001	0.001	0.001	
Cr	0.004	0.001	0.001	0.000	0.000	0.003	0.002	0.000	
Fe*	0.813	0.804	0.927	0.957	0.713	0.956	0.909	1.039	
Mn	0.012	0.009	0.023	0.018	0.015	0.027	0.019	0.007	
Mg	1.121	1.098	1.001	1.005	1.252	0.991	1.034	0.910	
Ca	0.017	0.037	0.018	0.016	0.013	0.019	0.020	0.016	
Na	0.001	0.000	0.007	0.000	0.002	0.000	0.000	0.003	
K	0.002	0.003	0.000	0.001	0.002	0.002	0.003	0.003	
Zn	0.001	0.000	0.003	0.001	0.001	0.000	0.001	0.003	
Total	4.002	3.990	4.006	4.011	4.020	4.009	4.001	3.997	
En	0.57	0.57	0.51	0.51	0.63	0.50	0.53	0.46	
Fs	0.42	0.41	0.48	0.48	0.36	0.49	0.46	0.53	
Wo	0.01	0.02	0.01	0.01	0.01	0.01	0.01	0.01	

plagioclase (number of oxygens = 8)									
Sample No.	A98021701A	B98012802D	B98012802H	B98020303C	A98022001K4	A98022001K4	A98022001K4	B98021108A	
Rock type	Type 1	Type 1	Type 2	Type 3	Type 4	Type 4	Type 4	Type 5	
					primary	secondary	lamella in Cpx		
SiO ₂	54.783	55.076	56.583	55.438	48.630	50.415	49.965	61.054	
Al ₂ O ₃	28.609	27.324	27.550	28.608	33.204	32.151	32.199	25.831	
TiO ₂	0.000	0.018	0.000	0.000	0.000	0.007	0.000	0.007	
Cr ₂ O ₃	0.000	0.006	0.015	0.000	0.000	0.000	0.000	0.000	
FeO*	0.055	0.118	0.342	0.000	0.124	0.211	0.176	0.160	
MnO	0.015	0.028	0.000	0.000	0.019	0.000	0.000	0.011	
MgO	0.000	0.019	0.021	0.000	0.037	0.009	0.000	0.011	
CaO	9.951	9.911	9.597	10.457	15.242	13.783	14.137	7.708	
Na ₂ O	5.329	5.942	6.147	5.833	2.666	3.447	3.328	6.802	
K ₂ O	0.304	0.289	0.138	0.304	0.127	0.097	0.073	0.291	
ZnO	0.006	0.000	0.021	0.000	0.047	0.000	0.000	0.000	
Total	99.052	98.731	100.414	100.640	100.096	100.120	99.878	101.875	
Si	2.487	2.515	2.535	2.485	2.221	2.291	2.279	2.670	
Al	1.530	1.470	1.455	1.511	1.787	1.722	1.731	1.331	
Ti	0.000	0.001	0.000	0.000	0.000	0.000	0.000	0.000	
Cr	0.000	0.000	0.001	0.000	0.000	0.000	0.000	0.000	
Fe*	0.002	0.005	0.013	0.000	0.005	0.008	0.007	0.006	
Mn	0.001	0.001	0.000	0.000	0.001	0.000	0.000	0.000	
Mg	0.000	0.001	0.001	0.000	0.003	0.001	0.000	0.001	
Ca	0.484	0.485	0.461	0.502	0.746	0.671	0.691	0.361	
Na	0.469	0.526	0.534	0.507	0.236	0.304	0.294	0.576	
K	0.018	0.017	0.008	0.017	0.007	0.006	0.004	0.016	
Zn	0.000	0.000	0.001	0.000	0.002	0.000	0.000	0.000	
Total	4.991	5.020	5.008	5.022	5.007	5.002	5.005	4.961	
An	0.50	0.47	0.46	0.49	0.75	0.68	0.70	0.38	
Ab	0.48	0.51	0.53	0.49	0.24	0.31	0.30	0.60	
Or	0.02	0.02	0.01	0.02	0.01	0.01	0.00	0.02	

*: Total Fe as FeO

in mafic granulites from Tonagh Island, Napier Complex.

clinopyroxene (number of oxygens = 6)									
A98021701A	B98012802D	B98012802H	B98020303C	B98020303C	A98022001K4	A98020916K	A98020916K	B98021108A	
Type 1	Type 1	Type 2	Type 3	Type 3	Type 4	Type 4	Type 4	Type 4	Type 5
			primary	secondary		host	lamella in Opx		
50.522	51.344	51.077	51.199	51.012	50.905	52.201	51.746	51.222	
2.221	2.424	2.498	2.523	2.519	2.988	1.458	1.948	1.857	
0.161	0.268	0.252	0.231	0.194	0.313	0.101	0.176	0.182	
0.359	0.051	0.076	0.007	0.063	0.000	0.211	0.266	0.062	
8.398	9.872	10.655	10.754	10.540	7.724	10.433	10.516	13.470	
0.214	0.201	0.278	0.153	0.082	0.150	0.330	0.374	0.153	
12.745	12.561	12.269	11.753	12.451	13.623	12.465	12.144	10.393	
21.399	22.193	22.310	22.212	22.187	22.442	22.104	22.151	21.540	
0.406	0.492	0.612	0.667	0.547	0.406	0.551	0.526	0.563	
0.046	0.000	0.055	0.089	0.071	0.032	0.009	0.046	0.039	
0.000	0.023	0.056	0.012	0.000	0.102	0.000	0.000	0.000	
96.471	99.429	100.138	99.600	99.666	98.685	99.863	99.893	99.481	
1.954	1.940	1.927	1.940	1.930	1.921	1.968	1.953	1.963	
0.101	0.108	0.111	0.113	0.112	0.133	0.065	0.087	0.084	
0.005	0.008	0.007	0.007	0.006	0.009	0.003	0.005	0.005	
0.011	0.002	0.002	0.000	0.002	0.000	0.006	0.008	0.002	
0.271	0.312	0.336	0.341	0.333	0.244	0.329	0.332	0.432	
0.007	0.006	0.009	0.005	0.003	0.005	0.011	0.012	0.005	
0.734	0.707	0.690	0.663	0.702	0.766	0.700	0.683	0.593	
0.886	0.898	0.902	0.901	0.899	0.907	0.892	0.895	0.884	
0.030	0.036	0.045	0.049	0.040	0.030	0.040	0.038	0.042	
0.002	0.000	0.003	0.004	0.003	0.002	0.000	0.002	0.002	
0.000	0.001	0.002	0.000	0.000	0.003	0.000	0.000	0.000	
4.002	4.016	4.033	4.024	4.029	4.019	4.014	4.015	4.011	
En	0.39	0.37	0.36	0.35	0.36	0.40	0.36	0.31	
Fs	0.14	0.16	0.17	0.18	0.17	0.13	0.17	0.23	
Wo	0.47	0.47	0.47	0.47	0.46	0.47	0.46	0.46	

hornblende (number of oxygens = 23)			garnet (number of oxygens = 12)				
B98012802H	B98020303C	B98021108A	B98020303C	A98022001K4	A98022001K4	B98021108A	
Type 2	Type 3	Type 5	Type 3	Type 4	Type 4	Type 5	
around Cpx	around Cpx				lamella in Opx		
43.629	41.744	41.609	38.334	38.679	38.564	38.170	
11.697	13.189	11.451	21.869	22.254	21.695	20.874	
0.137	0.219	1.867	0.006	0.000	0.065	0.010	
0.000	0.006	0.000	0.008	0.053	0.066	0.000	
16.945	16.728	18.868	28.040	24.482	25.876	30.409	
0.070	0.118	0.011	0.872	1.525	1.783	0.926	
10.829	10.226	8.161	4.362	6.412	5.225	3.059	
11.650	10.791	11.374	7.295	6.655	6.534	7.196	
0.706	1.312	1.398	0.027	0.015	0.000	0.000	
1.264	1.830	2.154	0.000	0.000	0.029	0.000	
0.010	0.000	0.000	0.022	0.013	0.000	0.049	
96.937	96.163	96.893	100.835	100.088	99.857	100.693	
6.581	6.382	6.418	2.990	2.990	3.014	3.018	
2.079	2.376	2.081	2.010	2.027	1.997	1.945	
0.016	0.025	0.216	0.000	0.000	0.004	0.001	
0.000	0.001	0.000	0.000	0.003	0.004	0.000	
2.137	2.138	2.433	1.828	1.582	1.690	2.010	
0.009	0.015	0.001	0.058	0.100	0.118	0.062	
2.433	2.329	1.875	0.507	0.738	0.608	0.360	
1.882	1.767	1.879	0.609	0.551	0.547	0.609	
0.206	0.389	0.418	0.004	0.002	0.000	0.000	
0.243	0.357	0.424	0.000	0.000	0.003	0.000	
0.001	0.000	0.000	0.001	0.001	0.000	0.003	
15.588	15.778	15.746	8.007	7.996	7.983	8.009	
XMg	0.53	0.52	Pyr	0.17	0.25	0.21	0.12
			Alm	0.61	0.53	0.57	0.66
			Grs	0.20	0.19	0.18	0.20
			Sps	0.02	0.03	0.04	0.02

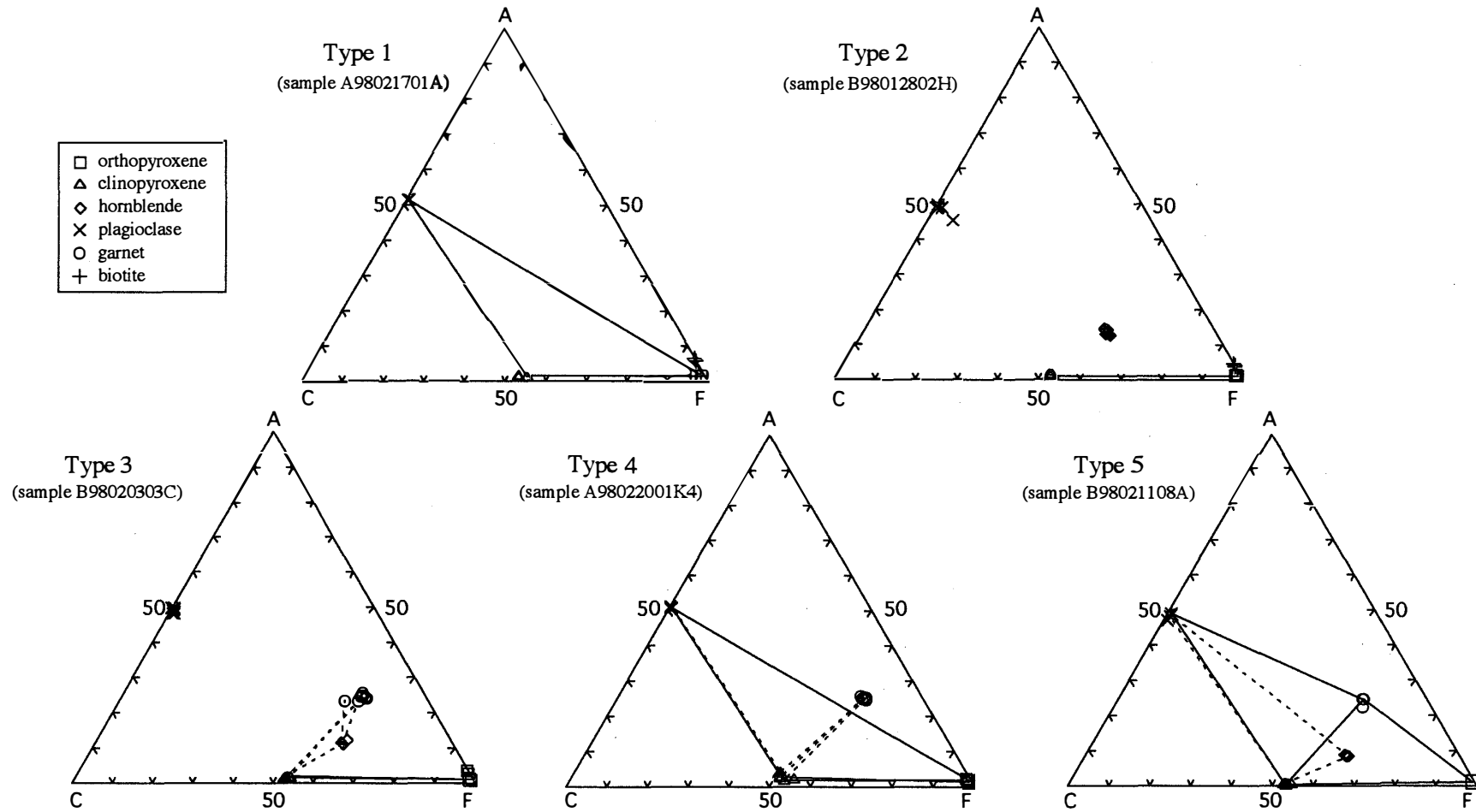


Fig. 3. ACF diagrams showing assemblages and compositions of minerals in mafic granulites from Tonagh Island, Napier Complex. Labels in the upper left denote numbers of rock types discussed in the text. Solid and broken tie lines in the diagrams of types 1 to 4 indicate primary and retrograde mineral assemblages, respectively. For type 5, solid and broken tie lines indicate mineral assemblages in garnet-rich and hornblende-rich portions, respectively.

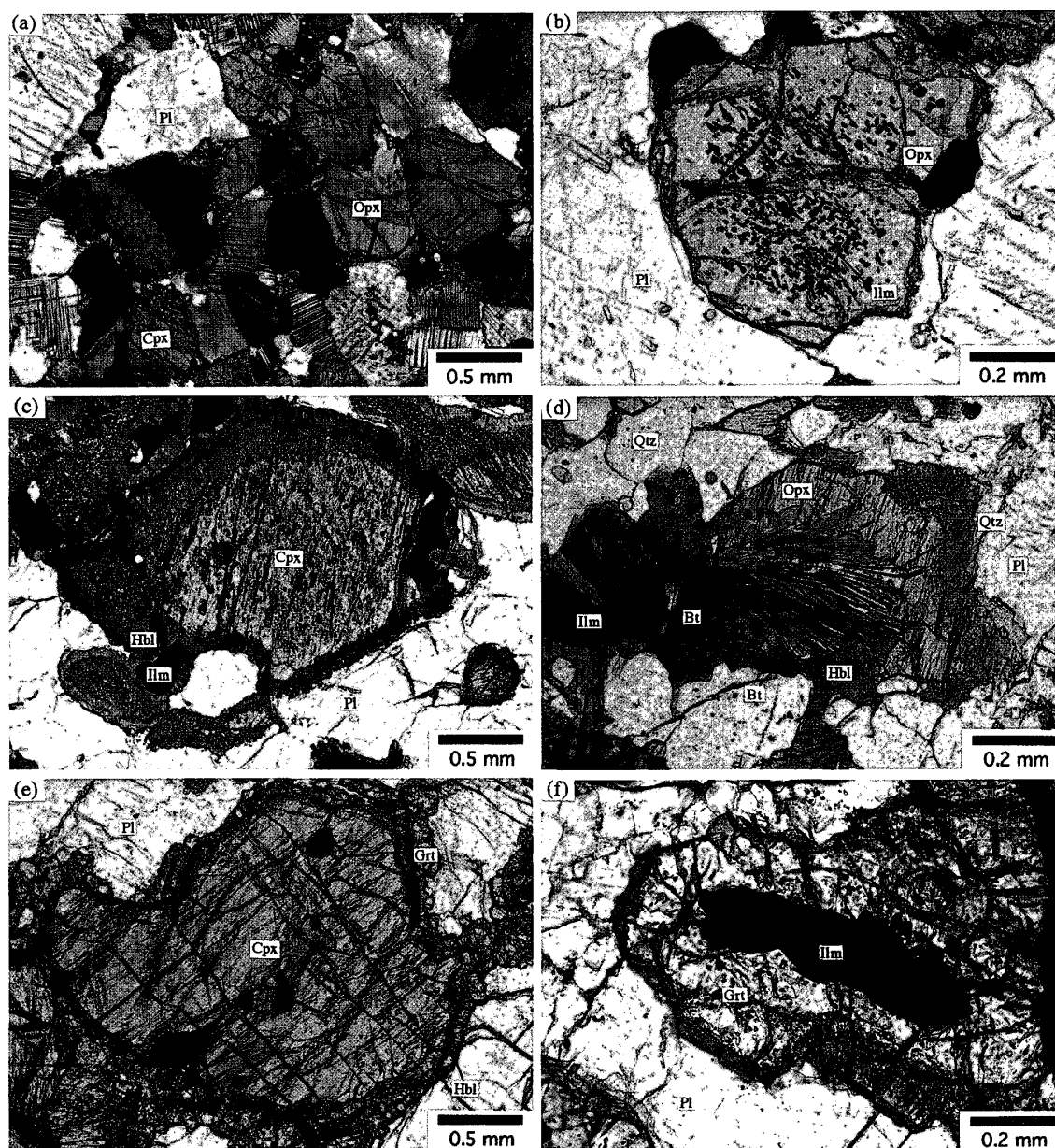


Fig. 4. Photomicrographs of mafic granulites.

(a) Medium-grained granoblastic texture of orthopyroxene, clinopyroxene, and plagioclase in type 1 mafic granulite (sample B98012802D, Unit II). Crossed polars. (b) Lamella of ilmenite in subhedral orthopyroxene as evidence of exsolution after peak metamorphism. It is abundant in the core of the orthopyroxene but almost absent toward the rim (sample B98012802D, Unit II). Polarized light. (c) Hornblende-quartz symplectite around clinopyroxene in type 2 mafic granulite (sample B98012802H, Unit II). The texture is evidence of retrograde hydration by infiltration of H_2O -bearing fluid. Polarized light. (d) Biotite-quartz symplectite around orthopyroxene in type 2 mafic granulite (sample B98012802H, Unit II). The texture suggests a retrograde interaction of melt and mafic granulite. Polarized light. (e) Garnet-hornblende corona around clinopyroxene in type 3 mafic granulite (sample B98020303C, Unit II). Polarized light. (f) Corona of garnet around ilmenite suggesting possible retrograde garnet-forming reaction (sample B98020303C, Unit II).

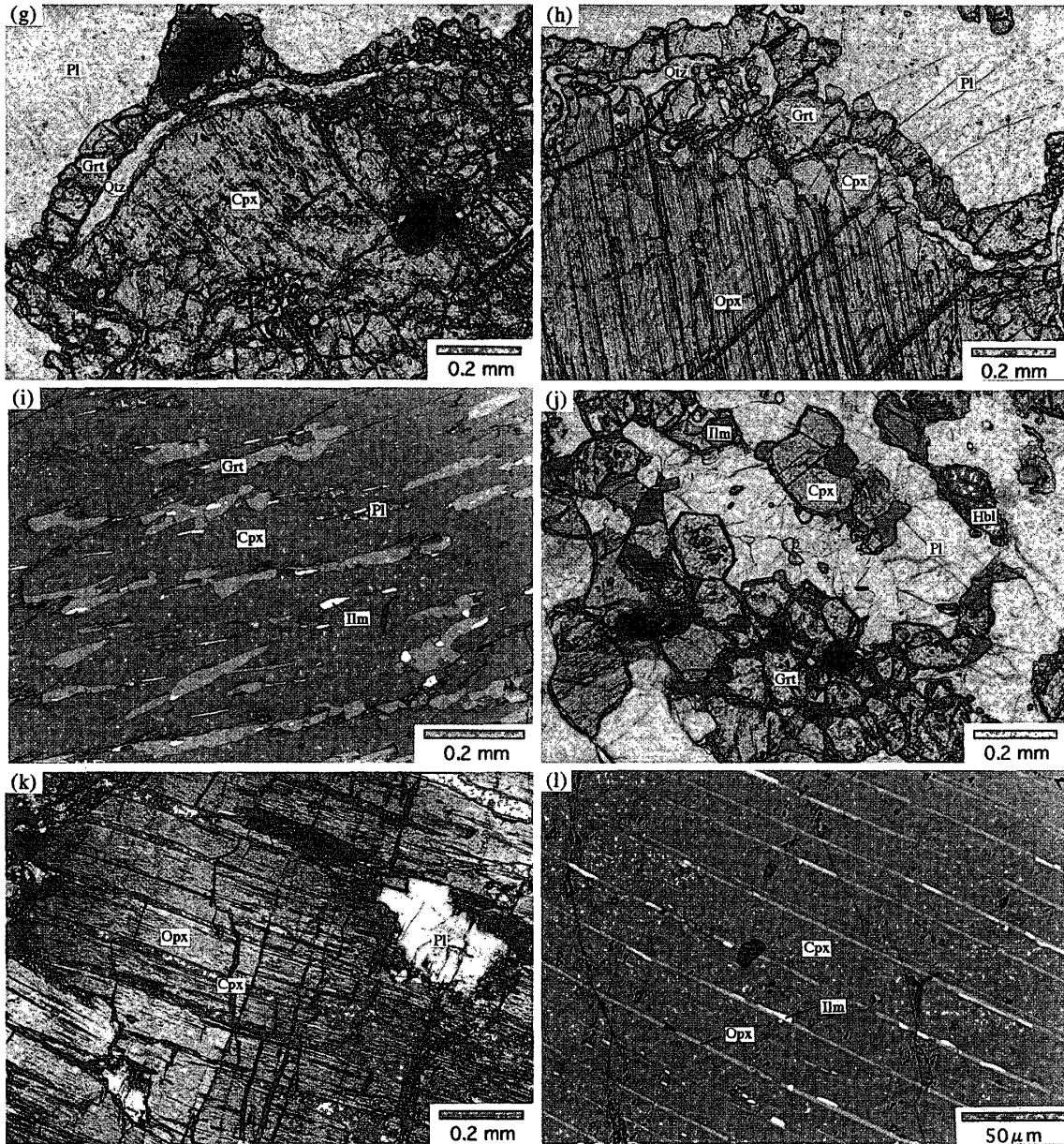


Fig. 4. (continued).

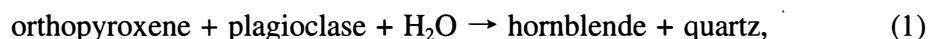
(g) Garnet-quartz corona around clinopyroxene in type 4 mafic granulite (sample A98020916B, Unit I). The texture is similar to that in Fig. 4e, but hornblende is not present in this sample. Polarized light. (h) Garnet-quartz-clinopyroxene corona around orthopyroxene in type 4 mafic granulite (sample A98020916B, Unit I). The texture is also an evidence of isobaric cooling after UHT metamorphism. Polarized light. (i) Back scattering image of clinopyroxene in type 4 mafic granulite (sample A98022001K4, Unit I). The clinopyroxene contains lamella of garnet, plagioclase, and ilmenite probably as a product of a retrograde event. (j) Fine-grained granoblastic texture of garnet-clinopyroxene-plagioclase-hornblende assemblage in type 5 mafic granulite (sample B98021108A, Unit III). The rock has suffered granulite-facies metamorphism after an intrusion of a protolith mafic dyke during the cooling stage. Polarized light. (k) Lamella of clinopyroxene in coarse-grained orthopyroxene in type 4 mafic granulite (sample A98020916K, Unit I). The orthopyroxene was originally pigeonite, but suffered exsolution during cooling and now compositionally hypersthene. Crossed polars. (l) Back scattering image of thin lamella of orthopyroxene in clinopyroxene in type 4 mafic granulite (sample A98020916K, Unit I).

content (An) in plagioclases of type 1 mafic granulite from Units I and V shows higher values (An50–82) than that from Unit II (An34–48) probably reflecting differences in bulk rock chemistry. It shows no compositional zoning pattern within single crystals.

Quartz is present in all samples, but not abundant. It occurs as small aggregates along grain boundaries of plagioclase and pyroxenes. Opaque minerals are mainly ilmenite and minor magnetite. Reddish-brown biotite ($X_{Mg}=0.66-0.77$) is a minor hydrous mineral. It is present as a retrograde phase rimming in part orthopyroxene and magnetite. Minor hornblende is present around pyroxenes in some samples, but its volume is less than 1 vol%.

3.2. Type 2: Two-pyroxene mafic granulite (with retrograde hornblende and quartz)

Type 2 mafic granulite, which occurs only in Unit II, also shows granoblastic texture of plagioclase and ortho- and clinopyroxenes. It is, however, different from type 1 because of the presence of hornblende-quartz coronas around ortho- and clinopyroxenes (Fig. 4c). Sample B98012802H, for example, is composed of plagioclase (An44–50), orthopyroxene ($X_{Mg}=0.51-0.53$), clinopyroxene ($X_{Mg}=0.67-0.68$), and greenish hornblende, with accessory quartz, ilmenite, magnetite, and biotite. The hornblende is >5 vol% and always rimming pyroxenes. The texture suggests that the following hydration reactions (1) and (2) took place.



Composition of hornblende varies from sample to sample, but is mainly edenite to pargasite according to the classification of LEAKE *et al.* (1997). There is no significant difference in chemistry of hornblende formed by the two reactions. Presence of irregular-shaped ilmenite associated with these coronas (Fig. 4c) suggests that the Ti-bearing phase exsolved from pyroxenes during the hydration reaction.

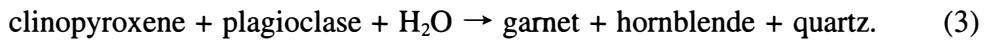
Modal abundances and textures of plagioclase and quartz are similar to those of type 1. Composition of plagioclase (An42–53 for all type 2 samples) is also similar to that in type 1 mafic granulite of Unit II, but slightly An-poor compared to that from Units I and V. As there is no significant difference in mineral chemistry of orthopyroxene, clinopyroxene, and plagioclase between type 1 and 2 mafic granulites, the presence of hornblende may be influenced by an elevation of activity of water ($a_{\text{H}_2\text{O}}$) by infiltration of H_2O -bearing fluid. Timing of the hydration is not known but is probably associated with retrograde metamorphism under amphibolite-facies condition.

In quartz- and biotite-rich portion of sample B98012802H, biotite-quartz symplectite is present around orthopyroxene (Fig. 4d). The texture may suggest an interaction between orthopyroxene and melt (*e.g.* RIDLEY, 1992).

3.3. Type 3: Two-pyroxene mafic granulite (with retrograde garnet, hornblende, and quartz)

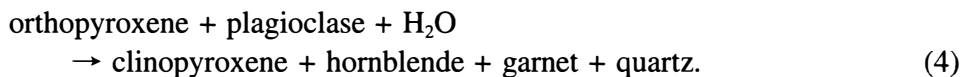
Type 3 mafic granulite occurs in a thick layer of mafic granulite in Unit II. It is characterized by the presence of retrograde hornblende, garnet, and minor amounts of quartz as well as primary plagioclase, orthopyroxene, and clinopyroxene. Ilmenite, magnetite, and apatite are accessory minerals.

Garnet is present as aggregates of small and subhedral grains surrounding clinopyroxene or hornblende-quartz coronas around clinopyroxene. Composition of the garnet is almandine-rich, $\text{Alm}_{61-63}\text{Pyr}_{15-17}\text{Grs}_{19-21}\text{Sps}_{2-3}$ for sample B98020303C, and shows little variation between samples. The texture suggests that the following hydration reaction (3) took place.



X_{Mg} of the reactant clinopyroxene is 0.64–0.72, which shows no compositional difference from those of types 1 and 2. Composition of plagioclase varies from samples to sample, being An42–45 for sample B98012801B and An42–50 for sample B98020303C. They are almost consistent with those in type 1 (An34–48; sample B98012802D) and type 2 (An44–50; sample B98012802H) mafic granulites of Unit II. Composition of hornblende is similar to that of type 2 as edenite.

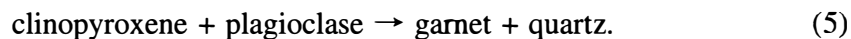
The retrograde garnet-hornblende-quartz corona is also present around orthopyroxene ($X_{\text{Mg}}=0.50-0.60$) in sample B98020303C. The texture is, however, different from that of reaction (3) because of the presence of fine-grained clinopyroxenes between orthopyroxene and corona. This suggests the following reaction (4).



Compositions of garnet and hornblende formed by the reaction are similar to those of reaction (3). As shown in Fig. 4f, garnet is also present as corona around ilmenite in some type 3 mafic granulites, suggesting a garnet-forming reaction including ilmenite.

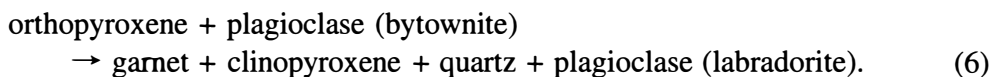
3.4. Type 4: Two-pyroxene mafic granulite (with retrograde garnet and quartz)

The type 4 mafic granulite is characterized by retrograde formation of garnet and quartz around ortho- and clinopyroxenes without hydrous minerals (Fig. 4g). Accessory minerals are ilmenite and magnetite. The rock type occurs mainly in Units I and V. In sample A98022001K4, all subhedral clinopyroxene ($X_{\text{Mg}}=0.73-0.78$) is surrounded by a corona of quartz and garnet ($\text{Alm}_{53-57}\text{Pyr}_{21-25}\text{Grs}_{18-20}\text{Sps}_{3-4}$). The texture suggests that the following vapor-absent reaction (5) took place.



Although the reaction texture is distinguished from that of reaction (3), grain size and chemistry of garnet are similar to those of type 3.

Orthopyroxene in the sample also exhibits corona texture of garnet and quartz. The texture is different from that in reaction (5) because of the presence of small-grained clinopyroxene between orthopyroxene and garnet (Fig. 4h), similar to that in reaction (4). Fine-grained vermicular clinopyroxene is also present as inclusions in the garnet. In some samples, small plagioclase grains crystallized with the corona. They show elevated albite content (An62–68) compared with primary plagioclase (An72–78). The texture is therefore explained by the following reaction (6).



Composition of the secondary clinopyroxene ($X_{Mg}=0.76-0.78$) is similar to that of early-formed crystals. Garnet formed by reaction (6) also shows no difference in chemistry from that of reaction (5).

Large clinopyroxene ($X_{Mg}=0.72$) in sample A98022001K4 contains lamella of garnet and plagioclase as well as ilmenite (Fig. 4i). Although compositions of the lamella garnet ($Alm_{57}Pyr_{21}Grs_{18}Sps_4$) are similar to those of corona, plagioclase is more albite-rich (An_{69-70}) than that of primary origin (An_{72-78}). ELLIS and GREEN (1985) reported lamella garnet exsolved from clinopyroxene in ultramafic granulite (garnet-clinopyroxenite) from the northern end of Wyers Ice Shelf, western shore of Amundsen Bay, as evidence of near-isobaric cooling after peak metamorphism. The present garnet-plagioclase exsolution in clinopyroxene may be a product of retrograde metamorphism similar to that reported by ELLIS and GREEN (1985).

3.5. Type 5: Fine-grained clinopyroxene-hornblende-garnet mafic granulite (metamorphosed mafic dyke)

The rock occurs as a dyke of about several tens of centimeters in thickness along a major shear zone which separates Unit II from Unit III (Fig. 1). Although the dyke crosscuts the gneissosity of surrounding gneisses and clearly postdates a major deformation event (Fig. 2b), it also suffered metamorphism together with adjacent rocks.

The type 5 mafic granulite shows fine-grained granoblastic texture except for the locally sheared sample. The rock is composed mainly of plagioclase, clinopyroxene, garnet, and hornblende (Fig. 4j). These minerals show little compositional variation between samples, probably because of similar bulk rock chemistry of protolith mafic dykes. Quartz, biotite, orthopyroxene, and ilmenite are accessory minerals.

Garnet in the sample consists of subhedral to euhedral crystals and is probably of primary origin. It is compositionally homogeneous, $Alm_{62-65}Pyr_{11-16}Grs_{19-22}Sps_{1-4}$, and show no compositional zoning pattern. The garnet usually coexists with clinopyroxene and plagioclase, forming a garnet-rich pinkish lens in a dark-brownish, hornblende-rich matrix. Colorless to pale greenish clinopyroxene ($X_{Mg}=0.62-0.71$) is abundant in the garnet-rich portion. Lamella of orthopyroxene and ilmenite are not present in the crystal. Subhedral orthopyroxene ($X_{Mg}=0.46-0.47$) is also present in the garnet-rich portion. Plagioclase is abundant in both garnet-rich and hornblende-rich portions. Its anorthite content is low (An_{32-41}) compared with that in the other rock types. Hornblende (pargasite) is subhedral and brownish in color. It is abundant in the matrix dark-brownish portion of the rock and locally coexists with garnet.

4. Discussion

4.1. Peak metamorphism

Although available petrographical data indicate that mafic granulites from Tonagh Island have suffered a significant effect of retrograde metamorphism, type 1 mafic granulite probably preserves the mineral assemblage of peak metamorphism because of its granoblastic texture and lack of retrograde reactions. Mineral chemistry and P - T condition of peak metamorphism are, however, completely reset by the retrograde event. The later homogenization of mineral chemistry is supported by a similarity in composi-

tions between fine-grained clinopyroxene aggregates formed by retrograde reactions and medium-grained primary clinopyroxene.

Evidence of UHT metamorphism in mafic granulites is preserved only in exsolution textures in pyroxenes. Sample A98020916K of type 4 mafic granulite shows exsolution of ortho- and clinopyroxenes (Fig. 4k and 4l). They are now compositionally hypersthene and augite, respectively (Table 2). Composition of primary pyroxenes at peak metamorphism was inferred considering the volume of host and lamella minerals. The result is $\text{En}_{48}\text{Fs}_{41}\text{Wo}_{11}$ for orthopyroxene (pigeonite) and $\text{En}_{37}\text{Fs}_{19}\text{Wo}_{44}$ for clinopyroxene (augite). Preliminary temperature estimates by two-pyroxene geothermometer indicate 900 and 980°C using the methods of WOOD and BANNO (1973) and WELLS (1977), respectively, suggesting a relic temperature of peak metamorphism.

4.2. Retrograde metamorphism

As discussed in the previous chapter, evidence of retrograde metamorphism is dominant in mafic granulites of Tonagh Island. Although some of the retrograde textures and reactions discussed above have already been observed by previous works on mafic and ultramafic granulites of the Napier Complex (*e.g.* ELLIS and GREEN, 1985; HARLEY, 1985; SHERATON *et al.*, 1987), this study has an advantage because many available textures and reactions in mafic granulite of the Napier Complex have been observed in the studied area. Mafic granulites of Tonagh Island are therefore useful to construct the retrograde history of the Napier Complex after UHT metamorphism.

Hornblende-quartz, biotite-quartz, and garnet-hornblende-quartz coronas after ortho- and clinopyroxenes are typical evidence of retrograde metamorphism at the amphibolite-facies conditions. The textures suggest that retrograde metamorphism took place by decreasing temperature in the presence of H_2O -bearing fluid.

Garnet-quartz corona after pyroxenes is a predominant retrograde texture throughout the studied area. As the univariant line of the reaction (5) shows a gentle slope in P - T space (*ca.* 100°C/kbar) and the garnet-quartz assemblage is stable on the low-temperature side of the line, temperature must have decreased nearly isobarically in the formation of garnet-quartz coronas (*e.g.* HARLEY, 1985).

Preliminary P - T estimates using garnet-clinopyroxene-plagioclase-quartz geothermobarometry (ELLIS and GREEN, 1979; MOECHER *et al.*, 1988) for sample B98012801B show very low temperature of 650–700°C at 6.5–8.0 kbar. The P - T data support the petrographical evidence that the retrograde metamorphism took place in the amphibolite-facies condition. It has to be noted that the isobaric cooling discussed above is significantly lower in temperature than the previously reported cooling temperature from 950°C subsequent to UHT metamorphism (*e.g.* SHERATON *et al.*, 1987). The present data therefore suggest that the second isobaric cooling (as low as 650°C) is distinguished from high-temperature isobaric cooling subsequent to UHT metamorphism.

Field occurrence of type 5 mafic granulite suggests that intrusion of protolith of the type 5 mafic granulite postdates a major tectonic event (Fig. 2b). Minor occurrence of orthopyroxene indicates that the mafic dyke has suffered an amphibolite-facies event which corresponds to retrograde metamorphism of Tonagh Island. P - T estimates from garnet-clinopyroxene-plagioclase-quartz assemblage in sample B98021504D show 630–670°C at 6.4–8.2 kbar, which are consistent with that of type 3 mafic granulite. The

condition therefore marks the last stage of regional metamorphism recorded in mafic granulites.

ISHIZUKA *et al.* (1998) reported two-pyroxene mafic granulite (clinopyroxene+plagioclase±quartz, orthopyroxene) from the Mt. Riiser-Larsen area of the Napier Complex. The mineral assemblage is petrographically similar to type 1 mafic granulite of this study. Lack of retrograde garnet implies that reactions (3) to (6) did not take place in mafic granulite from the Mt. Riiser-Larsen area. This may suggest higher-pressure retrograde metamorphism of Tonagh Island compared with the Mt. Riiser-Larsen area. Further investigations of reaction textures of mafic granulites from Amundsen Bay area are therefore a key to understand the retrograde uplifting history of the Napier Complex.

Acknowledgments

We express our sincere thanks to the members of JARE-39 and the crew of the icebreaker SHIRASE for giving us the opportunity for the geological field investigation, and their helpful support. Professors M. TAGIRI and T. OBA are acknowledged for critical reading of the manuscript.

References

- ELLIS, D.J. (1980): Osumilite-sapphirine-quartz granulites from Enderby Land, Antarctica: *P-T* conditions of metamorphism, implications for garnet-cordierite equilibria and the evolution of the deep crust. *Contrib. Mineral. Petrol.*, **74**, 201–210.
- ELLIS, D.J. and GREEN, D.D. (1979): An experimental study of the effect of Ca upon garnet-clinopyroxene Fe-Mg exchange equilibria. *Contrib. Mineral. Petrol.*, **71**, 13–22.
- ELLIS, D.J. and GREEN, D.H. (1985): Garnet-forming reactions in mafic granulites from Enderby Land, Antarctica—implications for geothermometry and geobarometry. *J. Petrol.*, **26**, 633–662.
- HARLEY, S.L. (1985): Garnet-orthopyroxene bearing granulites from Enderby Land, Antarctica: Metamorphic pressure-temperature-time evolution of the Archean Napier Complex. *J. Petrol.*, **26**, 819–856.
- HARLEY, S.L. (1987): A pyroxene-bearing meta-ironstone and other pyroxene-granulites from Tonagh Island, Enderby Land, Antarctica: Further evidence for very high temperature (>980°C) Archean regional metamorphism in the Napier Complex. *J. Metamorph. Geol.*, **5**, 341–356.
- ISHIZUKA, H., ISHIKAWA, M., HOKADA, T. and SUZUKI, S. (1998): Geology of the Mt. Riiser-Larsen area of the Napier Complex, Enderby Land, East Antarctica. *Polar Geosci.*, **11**, 154–171.
- KRETZ, R. (1983): Symbols for rock-forming minerals. *Am. Mineral.*, **68**, 277–279.
- LEAKE, B.E., WOOLLEY, A.R., ARPS, C.E.S., BIRCH, W.D., GILBERT, M.C., GRICE, J.D., HAWTHORNE, F.C., KATO, A., KISCH, H.J., KRIVOVICHEV, V.G., LINTHOUT, K., LAIRD, J., MANDARINO, J., MARESCH, W.V., NICKEL, E.H., ROCK, N.M.S., SCHUMACHER, J.C., SMITH, D.C., STEPHENSON, N.C.N., UNGARETTI, L., WHITTAKER, E.J.W. and YOUZHI, G. (1997): Nomenclature of amphiboles: Report of the subcommittee on amphiboles of the International Mineralogical Association, commission on new minerals and mineral names. *Am. Mineral.*, **82**, 1019–1037.
- MOECHER, D.P., ESSENE, E.J. and ANOVITZ, L.M. (1988): Calculation and application of clinopyroxene-garnet-plagioclase-quartz geobarometers. *Contrib. Mineral. Petrol.*, **100**, 92–106.
- OSANAI, Y., TOYOSHIMA, T., OWADA, M., TSUNOGAE, T., HOKADA, T. and CROWE, W.A. (1999): Geology of ultrahigh-temperature metamorphic rocks from Tonagh Island in the Napier Complex, East Antarctica. *Polar Geosci.*, **12**, 1–28.
- RIDLEY, J. (1992): On the origins and tectonic significance of the charnockite suite of the Archean Limpopo Belt, Northern Marginal Zone, Zimbabwe. *Precambrian Res.*, **55**, 407–427.

- SANDIFORD, M. and POWELL, R. (1986): Pyroxene exsolution in granulites from Fyfe Hills, Enderby Land, Antarctica: Evidence for 1000°C metamorphic temperatures in Archean continental crust. *Am. Mineral.*, **71**, 946–954.
- SHERATON, J.W., TINGEY, R.J., BLACK, L.P., OFFE, L.A. and ELLIS, D.J. (1987): Geology of an unusual Precambrian high-grade metamorphic terrane—Enderby Land and western Kemp Land, Antarctica. *BMR Bull.*, **223**, 51 p.
- TOYOSHIMA, T., OSANAI, Y., OWADA, M., TSUNOGAE, T., HOKADA, T. and CROWE, W.A. (1999): Deformation of ultrahigh-temperature metamorphic rocks from Tonagh Island in the Napier Complex, East Antarctica. *Polar Geosci.*, **12**, 29–48.
- WELLS, P.R.A. (1977): Pyroxene thermometry in simple and complex systems. *Contrib. Mineral. Petrol.*, **62**, 129–139.
- WOOD, B.J. and BANNO, S. (1973): Garnet-orthopyroxene and orthopyroxene-clinopyroxene relationships in simple and complex systems. *Contrib. Mineral. Petrol.*, **42**, 109–124.

(Received March 1, 1999; Revised manuscript accepted June 1, 1999)